Proper Orthogonal Decomposition Extensions For Parametric Applications in Transonic Aerodynamics

T. Bui-Thanh*, M. Damodaran†
Singapore-Massachusetts Institute of Technology Alliance (SMA)
School of Mechanical and Production Engineering
Nanyang Technological University, Nanyang Avenue, Singapore 639798
K. Willcox‡
Aerospace Computational Design Laboratory
Massachusetts Institute of Technology, Cambridge, MA 02139

Abstract

Two extensions to the proper orthogonal decomposition (POD) technique are considered for steady aerodynamic applications. The first is to couple the POD approach with a cubic spline interpolation procedure in order to develop fast, low-order models that accurately capture the variation in parameters, such as the angle of attack or inflow Mach number. The second extension is a "gappy" POD technique for the reconstruction of incomplete or inaccurate aerodynamic data. Gappy POD is shown to be an effective technique for reconstruction of full flow field data from limited surface measurements, and thus provides an effective way to combine experimental and computational data. A modification of the gappy POD is also shown to provide a simple, effective method for airfoil inverse design.

Introduction

The proper orthogonal decomposition (POD), also known as Karhunen Loéve expansion and principle components analysis, has been widely used for a broad range of applications. POD analysis yields a set of empirical eigenfunctions, which describes the dominant behavior or dynamics of given problem. This technique can be used for a variety of applications, including derivation of reduced-order dynamical models,[1] steady analysis and design of inviscid airfoils,[2] image processing,[3] and pattern recognition.[4]

Sirovich introduced the method of snapshots as a way to efficiently determine the POD eigenfunctions for large problems.[5] In particular, the method of snapshots has been widely applied to computational fluid dynamic (CFD) formulations to obtain reduced-order models for unsteady aerodynamic applications.[6–9] A set of instantaneous flow solutions, or "snapshots" are obtained from a simulation of the CFD method. The POD process then computes a set of eigenfunctions from these snapshots, which is optimal in the sense that, for any given basis size, the error between the original and reconstructed data is minimized. Reduced-order models can be derived by projecting the CFD model onto the reduced space spanned by the POD eigenfunctions.

While use of POD to capture the time variation of fluid dynamic problems has been widespread, the development of reduced-order models to capture parametric variation is less common. The POD has been used to develop reduced-order models for turbomachinery flows with sampling in both time and over a range of interblade phase angles.[10] The resulting models were applied to flows at varying Mach numbers, although the snapshot ensemble is computed at a single Mach number condition. Accurate results were obtained for Mach numbers close to that used in the snapshots. The POD has also been used to develop models for optimization purposes.[2] In this case, the POD modes span a range of airfoil geometries. In another example that includes parametric variation, a fast computation has been developed that uses a POD basis to predict the steady-state temperature distribution of flow in a square cavity as the Rayleigh number is varied.[11] This method is a simple combination of the POD basis and an interpolation procedure.

A different application of the POD is for the repair of damaged data and construction of missing or "gappy" data as introduced in Everson and Sirovich[12] for the characterization of human faces. This idea could be extended to the prediction of aerodynamic flow fields. For example, a set of complete flow solutions may be available from a CFD calculation. One might wish to use these solutions as an information database in the reconstruction of partial data, such as that obtained from experimental measurements.

In this paper, two extensions to the POD for aerodynamic applications will be considered. The first is to combine the POD approach with a cubic spline interpolation to capture parametric variations. The second application will apply the gappy POD for data reconstruction of aerodynamic flows. The paper is structured as follows. The basic POD method is first

*SMA Graduate Research student
†Associate Professor, Associate Fellow AIAA
‡Assistant Professor of Aeronautics and Astronautics, Member AIAA

outlined, followed by a description of the extensions with interpolation and incomplete data sets. A set of results will then be presented. The first example considers steady transonic flow past an airfoil with varying angle of attack and Mach number. Next, using gappy POD, cases are presented in which a complete flow pressure field is reconstructed from surface pressure values and the POD snapshots are constructed from an incomplete set of aerodynamic data. Finally, the gappy POD inverse design approach is demonstrated for a variety of subsonic airfoils.

Proper Orthogonal Decomposition Theory and Extensions

Proper orthogonal decomposition

The basic POD procedure is summarized briefly here. The optimal POD basis vectors Φ are chosen to maximize the cost:[1]

$$\max_{\Psi} \frac{\left\langle \left| (U,\Psi)^2 \right| \right\rangle}{(\Psi,\Psi)} = \frac{\left\langle \left| (U,\Phi)^2 \right| \right\rangle}{(\Phi,\Phi)} \tag{1}$$

where (U,Φ) is the inner product of the basis vector Φ with the field $U(x,t)$, x represents the spatial coordinates, t is the time, and $<>$ is the time-averaging operation. It can be shown that the POD basis vectors are eigenfunctions of the kernel K given by

$$K(x,x') = \langle U(x,t), U^*(x',t) \rangle \tag{2}$$

The method of snapshots, introduced by Sirovich,[5] is a way of finding the eigenfunctions Φ without explicitly calculating the kernel K. Consider an ensemble of instantaneous solutions, or "snapshots". It can be shown that the eigenfunctions of K are linear combination of the snapshots as follows

$$\Phi = \sum_{i=1}^{m} \beta_i U^i \tag{3}$$

where U^i is the solution at a time t_i and the number of snapshots, m, is large. For fluid dynamic applications, the vector U^i contains the flow unknowns at each point in the computational grid. The coefficients β_i can be shown to satisfy the eigen-problem

$$R\beta = \Lambda\beta \tag{4}$$

where R is known as the correlation matrix

$$R_{ik} = \frac{1}{m}\left(U^i, U^k\right) \tag{5}$$

The eigenvectors of R determine how to construct the POD basis vectors [using (3)], while the eigenvalues of R determine the importance of the basis vectors. The relative "energy" (measured by the 2-norm) captured by the i^{th} basis vector is given by $\lambda_i / \sum_{j=1}^{m} \lambda_j$. The approximate prediction of the field U is then given by a linear combination of the eigenfunctions

$$U \approx \sum_{i=1}^{p} \alpha_i \Phi^i \tag{6}$$

where $p << m$ is chosen to capture the desired level of energy, Φ^i is the i^{th} POD basis vector, and the POD coefficients α_i must be determined as a function of time.

POD with interpolation

The basic POD procedure outlined in the previous section considered time-varying flows by taking a series of flow solutions at different instants in time. The procedure could also be applied in parameter space as in Epureanu et al.,[10] that is, obtaining flow snapshots while allowing a parameter to vary. Assume that the parameter of interest is denoted by δ. This could, for example, be the flow freestream Mach number or airfoil angle of attack.

A procedure for rapid prediction of the flow solution U at any value of δ is as follows:

1. Let $\left\{U^{\delta_i}\right\}_{i=1}^{m}$ be the set of snapshots corresponding to the set of parameter values $\{\delta_i\}_{i=1}^{m}$.

2. Perform the basic POD procedure described above on $\left\{U^{\delta_i}\right\}_{i=1}^{m}$ to get the orthonormal POD basis $\left\{\Phi^k\right\}_{k=1}^{m}$.

3. The reconstruction of each snapshot is given by

$$U^{\delta_i} = \sum_{j=1}^{p} \alpha_j^{\delta_i} \Phi^j \tag{7}$$

   where $p < m$ is the number of eigenfunctions used in the reconstruction. The POD coefficients $\alpha_j^{\delta_i}$ are given by

$$\alpha_j^{\delta_i} = \left(\Phi^j, U^{\delta_i}\right) \tag{8}$$

4. If $\left\{\alpha_j^{\delta_i}\right\}_{i=1}^{m}$ is a smooth function of δ, interpolation can be used to determine the POD coefficients for intermediate values of δ that were not included in the original ensemble. The prediction of U^{δ} at any value of δ via the POD expansion is given by (6)

$$U^{\delta} = \sum_{j=1}^{p} \alpha_j^{\delta} \Phi^j \tag{9}$$

   where the coefficients α_j^{δ} are found by cubic spline interpolation of the set $\left\{\alpha_j^{\delta_i}\right\}_{i=1}^{m}$. Note that no discussion of a smoothness requirement was given by Hung;[11] however, this is important for the interpolation result to be reliable.

Gappy POD for reconstruction of missing data

In CFD applications, the POD has predominantly been used for deriving reduced-order models via projection of the governing equations onto the reduced space spanned by the basis vectors. Here, we consider a different application of the method, which is based on the gappy POD procedure developed by Everson and Sirovich[12] for the reconstruction of human face images from incomplete data sets. In this paper, the gappy POD methodology will be extended for consideration of fluid dynamic applications. The gappy POD procedure is first described.

The first step is to define a "mask" vector, which describes for a particular flow vector where data is available and where data is missing. For the flow solution U^k, the corresponding mask vector n^k is defined as follows:

$$\begin{aligned} n_i^k &= 0 \text{ if } U_i^k \text{ is missing or incorrect} \\ n_i^k &= 1 \text{ if } U_i^k \text{ is known} \end{aligned}$$

where U_i^k denotes the i^{th} element of the vector U^k. For convenience in formulation and programming, zero values are assigned to the elements of the vector U^k where the data is missing, and pointwise multiplication is defined as $\left(n^k, U^k\right)_i = n_i^k U_i^k$. Then the gappy inner product is defined as $(u,v)_n = ((n,u),(n,v))$, and the induced norm is $(\|v\|_n)^2 = (v,v)_n$.

Let $\left\{\Phi^i\right\}_{i=1}^m$ be the POD basis for the snapshot set $\left\{U^i\right\}_{i=1}^m$, where all snapshots are completely known. Let g be another solution vector that has some elements missing, with corresponding mask vector n. Assume that there is a need to reconstruct the full or "repaired" vector from the incomplete vector g. Assuming that the vector g represents a solution whose behavior can be characterized with the existing snapshot set, an expansion of the form (6) can be used to represent the intermediate repaired vector $\tilde{g}$ in terms of p POD basis functions as follows:

$$\tilde{g} \approx \sum_{i=1}^{p} b_i \Phi^i \tag{10}$$

To compute the POD coefficients b_i, the error, E, between the original and repaired vectors must be minimized. The error is defined as

$$E = \|g - \tilde{g}\|_n^2 \tag{11}$$

using the gappy norm so that only the original existing data elements in g are compared. The coefficients b_i that minimize the error E can be found by differentiating (11) with respect to each of the b_i in turn. This leads to the linear system of equations

$$Mb = f \tag{12}$$

where $M_{ij} = \left(\Phi^i, \Phi^j\right)_n$ and $f_i = \left(g, \Phi^i\right)_n$. Solving equation (12) for b and using (10), the intermediate repaired vector $\tilde{g}$ can be obtained. Finally, the complete g is reconstructed by replacing the missing elements in g by the corresponding repaired elements in $\tilde{g}$, i.e. $g_i = \tilde{g}_i$ if $n_i = 0$.

Gappy POD with an incomplete snapshot set

The gappy POD procedure can be extended to the case where the snapshots themselves are not completely known. In this case, the POD basis can be constructed using an iterative procedure. Consider a collection of incomplete data $\left\{g^k\right\}_{k=1}^m$, with an associated set of masks $\left\{n^k\right\}_{k=1}^m$. The first step is to fill in the missing elements of the snapshots using average values as follows:

$$h_i^k(0) = \begin{cases} g_i^k & \text{if } n_i^k = 1 \\ \bar{g}_i & \text{if } n_i^k = 0 \end{cases} \tag{13}$$

where $\bar{g}_i = \frac{1}{P_i}\sum_{k=1}^m g_i^k$, $P_i = \sum_{k=1}^m n_i^k$ and $h^k(l)$ denotes the l^{th} iterative guess for the vector h^k. A set of POD basis vectors can now be computed for this snapshot set, and iteratively used to refine the guess for the incomplete data. The procedure can be summarized as follows, beginning with $l = 0$:

1. Use the basic POD procedure on the snapshot set $\left\{h^k(l)\right\}_{k=1}^m$ to obtain the POD basis vectors for the current iteration, $\left\{\Phi^k(l)\right\}_{k=1}^m$.

2. Use the first p of these POD basis vectors to repair each member of the snapshot ensemble, as described in the previous section. The intermediate repaired data for the current iteration is given by
$$\tilde{h}^k(l) = \sum_{i=1}^{p} b_i^k(l)\Phi^i(l) \tag{14}$$

3. The values from these intermediate repaired data are now used to reconstruct the missing data for the next iteration as follows
$$h_i^k(l+1) = \begin{cases} h_i^k(l) & \text{if } n_i^k = 1 \\ \tilde{h}_i^k(l) & \text{if } n_i^k = 0 \end{cases} \tag{15}$$

4. Set $l = l + 1$ and go to step 1.

The above iterative procedure should be repeated until the maximum number of iterations is reached or until the algorithm has converged. When evaluating convergence, one can consider both the POD eigenvalues and the POD eigenvectors as will be demonstrated in the results.

Inverse Design via the Gappy POD Method

We now describe how the gappy POD method can be extended for fluid dynamic applications. In particular, a new variant of the method is proposed to perform inverse design of a two-dimensional airfoil. Typically,

given a target pressure distribution P^*, the inverse design problem is to find an optimal airfoil shape whose surface pressure distribution P minimizes the cost

$$J = \|P^* - P\|_2^2 \tag{16}$$

In order to solve this inverse design problem using the gappy POD method, the snapshots are first redefined. Rather than containing only flow variables, each snapshot is augmented to also contain airfoil coordinates. For example, consider the augmented snapshot set, $\{V^i\}_{i=1}^m$, where each snapshot contains a surface pressure distribution P^i and corresponding set of airfoil coordinates C^i:

$$V^i = \begin{bmatrix} C^i \\ P^i \end{bmatrix} \tag{17}$$

The target vector $V^* = [C^{*T}\ P^{*T}]^T$ can then be considered as an incomplete data vector, where P^* is known and C^* must be determined. Thus, the gappy POD procedure can be used to determine the optimal airfoil shape, using the procedure outlined in the previous section and minimizing the cost in (16) with respect to the gappy norm

$$J = \|V^* - \tilde{V}\|_n^2 \tag{18}$$

where n is the mask vector corresponding to V^* and the intermediate repaired vector $\tilde{V}$ is represented by a linear combination of basis vectors as in (10).

The inverse design problem has thus been converted into a problem of reconstructing missing data. In order to determine the airfoil shape, a system of linear equations must be solved, with size equal to the number of POD basis functions. The gappy POD method will then produce not only the optimal airfoil shape, but also the corresponding surface pressure distribution. If further flowfield information is desired, such as pressure distribution off the surface or other flow variables, this data could also be included in the augmented snapshot set.

The POD eigenvalues give guidance as to how many POD eigenfunctions should be included in the basis. Typically, one will include p basis vectors so that the relative energy captured, $\sum_{i=1}^p \lambda_i / \sum_{j=1}^m \lambda_j$, is greater than some threshold, typically taken to be 99% or higher. This energy measure determines how accurately a snapshot in the original ensemble can be reconstructed using the POD basis; however, it does not give any information regarding the accuracy of reconstructing a new vector. In the inverse design problem stated above, it is therefore important to monitor the value of the cost function J. One may choose enough POD basis functions to capture 99% or more of the snapshot energy, but the optimal value of J remains unacceptably high. This indicates that the subspace spanned by the chosen snapshots is not sufficiently rich to capture the desired design airfoil. Approaches for addressing this issue will be presented in the results section, which now follows.

Results and Discussion

Results will be presented for a variety of cases to demonstrate the interpolation and data reconstruction techniques. Snapshots were obtained from an inviscid steady-state CFD code, which uses a finite volume formulation as presented in Jameson et al.[13]

POD with interpolation for parametric variation

The first problem considered is steady flow about a NACA 0012 with varying angle of attack and Mach number. The Mach number interval [0.75, 0.85] is divided into 20 uniform intervals, and the angle of attack interval $[0°, 1.25°]$ is divided into 10 uniform intervals. Hence, the total number of snapshots in the ensemble is 231. Based on this snapshot set, interpolation will be used to predict the flow at any arbitrary Mach number and angle of attack within the range considered. For demonstration, POD will be applied to the pressure field only; the procedure for the other flow fields is straightforward.

The first prediction considered is for the pair ($\alpha = 0.45,\ M = 0.8$), in which $M = 0.8$ is one of the values used to generate the snapshots but $\alpha = 0.45$ is not. Figure 1 shows the comparison between the predicted pressure contours and the CFD pressure contours for this case. It can be seen in Figure 1(a) that with five eigenfunctions, the error is large in places and the two sets of contours are far apart. However, in Figure 1(c), as the number of POD basis vectors is increased to 25 the contours match closely. It should be noted that the cost for pressure prediction with 20, as in Figure 1(b), or 25 eigenfunctions does not differ greatly, since the method requires only interpolation of the scalar POD coefficients. The number of eigenfunctions can therefore be increased to obtain the desired level of accuracy.

The quality of the prediction is assessed by comparing the respective elements of the CFD solution and the solution reconstructed with p POD modes. Figure 2(a) shows the maximum percentage element error in log scale versus the number of POD modes used. It can be seen that the error decreases very quickly as number of eigenfunctions is increased from one to 25.

The second prediction considered is for the pair ($\alpha = 0.5,\ M = 0.812$), in which $\alpha = 0.5$ is one of the values used to generate the snapshots but $M = 0.812$ is not. Figure 3 shows the comparison between the predicted and CFD pressure contours. In general, it is observed that prediction is more sensitive to Mach number than angle of attack, hence it is expected that more eigenfunctions will be needed in this example to get a satisfactory result. As shown in Figures 3(c) and 2(b), 30 eigenfunctions are needed to achieve the desired level of accuracy.

The last example in this section is the prediction for the pair ($\alpha = 0.45, M = 0.812$) in which neither $\alpha = 0.45$ nor $M = 0.812$ are values used to generate the snapshots. Therefore, it is expected that a higher number of eigenfunctions will be needed to obtain a satisfactory result. Figure 4 shows the comparison between the predicted and CFD pressure contours for this case. As expected, it can be seen in Figure 2(c) and Figure 4 that more POD modes are required in this case. With 40 modes, a satisfactory level of accuracy is achieved.

The above results show that the POD method combined with interpolation allows models to be derived that accurately predict steady-state pressure fields over a range of parameter values. The approach can be extended to the case where more than two parameters vary. For example, one might wish to include geometric properties of the airfoil in order to apply these models in an optimization context. While the number of snapshots in this case might be large, the method presented in this paper is straightforward to apply.

Reconstruction of flowfield data

The NACA 0012 airfoil is considered at a freestream Mach number of 0.8. To create the POD basis, 51 snapshots are computed at uniformly spaced values of angle of attack in the interval $\alpha = [-1.25°, 1.25°]$ with a step of 0.05°. An incomplete flowfield was then generated by computing the flow solution at $\alpha = 0.77°$ (which is not one of the snapshots), and then retaining only the pressure values on the surface of the airfoil. The total number of pressure values in the full flowfield is 6369 and the number of pressure values on the airfoil surface is 121, hence 98.1% of the data is missing. The goal, then, is to reconstruct the full pressure flowfield using the gappy POD method. Such a problem might occur, for example, when analyzing experimental data. Typically, experimental measurements will provide only the airfoil surface pressure distribution; the gappy POD method provides a way to combine this experimental data with computational results in order to reconstruct the entire flowfield. In the case considered, the measurement points are evenly distributed over the airfoil surface. Figures 5(a) and (b) show the reconstructed pressure contours with four and five POD eigenfunctions, respectively, compared with the original contours of the CFD solution. As expected, the more eigenfunctions used, the more accurate is the reconstruction. With just limited surface pressure data available, the complete pressure field can be determined very accurately with only five POD eigenfunctions, showing that the gappy POD methodology for data reconstruction works effectively for an aerodynamic application.

A question of interest is whether the full pressure field can be accurately reconstructed with less surface data points available. Figure 5(c) shows the 2-norm of the error between the exact and reconstructed pressure field for four different cases. In each case, the number of available surface measurements is evenly distributed around the airfoil surface. It can be seen from Figure 5(c) that even when only 31 surface pressure measurements are available, the full pressure field can be constructed accurately with on the order of ten POD eigenmodes. When only 16 measurements are available, the result becomes unreliable.

Incomplete snapshot set

In the next example, the creation of a set of POD basis vectors from an incomplete set of snapshots is investigated. This problem may again be of interest if partial flowfield data is available from experimental results. Using the gappy POD methodology, experimental and computational data with differing levels of resolution can be combined effectively to determine dominant flow modes.

Again, we consider the NACA 0012 airfoil at a freestream Mach number of 0.8. A 26-member snapshot ensemble is used, corresponding to steady pressure solutions at angles of attack in the range $\alpha = [0°, 1.25°]$, uniformly spaced with an interval of 0.05°. To create the incomplete snapshot set for this example, 30% of the pressure data of each snapshot is discarded randomly. The algorithm described in the theory is then used to repair the data as follows. By first repairing the missing data points in each snapshot with the average over available data at that point, a new ensemble of data is created that has no missing values. With this new ensemble, a first approximation to the POD basis is then constructed. Then, each snapshot in the ensemble is repaired using the first approximation of the POD basis. This repaired ensemble is then used to construct a second approximation to the POD basis. For the example in this section, the iterative procedure above is stopped after 50 iterations.

In Figure 6, the second snapshot with 30% data missing is repaired by the above procedure with five POD eigenfunctions, which contain 99.99% of the flow energy. Figure 6(a) shows the original damaged snapshot. After one iteration, the repaired snapshot in Figure 6(b) begins to resemble the CFD solution; however, a large error remains. Figure 6(c) shows the repaired snapshot after 25 iterations and can be seen to match closely with the original. Figure 7 shows the repairing process for the 23^{rd} snapshot. Compared to the contours with 30% data missing in Figure 7(a), the reconstruction in Figure 7(c) is already close to the CFD result with only seven iterations. It can be seen that the convergence of the reconstruction process depends on the details of the particular snapshot under consideration. In particular, it depends on the structure of the flow snapshot and how much data is missing. For the 23^{rd} snapshot shown in Figure 7, the

convergence rate is much faster than for the second snapshot shown in Figure 6.

The convergence of the POD eigenvalue spectrum of the incomplete ensemble is shown in Figure 8. It can be seen that after one iteration the first two eigenvalues have converged, while convergence of subsequent eigenvalues requires more iterations. For example, after 45 iterations, it can be seen that only the first five eigenvalues have converged; however, these five modes account for almost all of the flow energy (99.99%).

Finally, we comment on the computational cost of the iterative gappy POD procedure. At each iteration, in order to reconstruct m snapshots, m systems of the form (12) must be solved. Furthermore, at each iteration, an eigenvalue problem of size m must be solved to determine the POD eigenfunctions. Using a 1.6 GHz Pentium 4 personal computer, with five POD eigenfunctions each iteration took less than two seconds.

Inverse Design Problem

The final set of examples demonstrates how the gappy POD method can be applied to the problem of inverse airfoil design. A collection of snapshots is generated as in (17) by choosing a set of airfoil shapes and obtaining their corresponding surface pressure distributions. (Other aspects of the flowfield could also be included if they are of interest.) While in this paper, CFD results were used to create the snapshots, in practice, the flow data could be obtained from computational simulations, experimental results, tabulated data, or a combination thereof. The goal, then, is to use the gappy POD method to determine the optimal airfoil shape that produces a given target pressure distribution, which is not contained in the snapshot collection.

Snapshots for subsonic airfoil design are created by considering the RAE 2822 airfoil and adding a series of Hicks-Henne bump functions,[14] which make smooth changes in the geometry. Thirty one bump functions were added to each of the upper and lower surfaces of the RAE 2822 airfoil to create a total of 63 airfoil snapshots, some of which are shown in Figure 9(a). The flow solutions for these airfoils were computed using the CFD model with zero angle of attack and a freestream Mach number of 0.5.

The pressure distribution for the Korn airfoil, whose geometry is also shown in Figure 9(a), is specified as the first design target. It can be seen in Figure 9(a) that, while the Korn airfoil shares some similarities with the RAE 2822-based snapshot set, its camber and thickness distribution are quite distinct. This example thus represents a challenge for the gappy POD inverse design methodology. The first 32 POD eigenvalues corresponding to the snapshot set are shown in Figure 9(b). It can be seen that the first 21 POD modes contain 99% of the system energy. Figure 10(a) shows the points on the Korn airfoil where target pressure values are specified. Using the gappy POD procedure, the corresponding optimal airfoil shape can then be determined. Figures 10(b), (c) and (d) compare the exact Korn airfoil and the target pressure to the POD design results using one, 15 and 29 eigenfunctions, respectively. It can be seen that as the number of eigenfunctions is increased, the predicted shape and its pressure distribution agree more closely with the exact solutions. The corresponding values of the cost J are given in Table 1. Using 29 POD modes, which account for 99.97% of the snapshot energy, it can be seen that the error in the pressure distribution is very small.

Using the same ensemble of snapshots as in the previous case, three different target pressure distributions were considered, corresponding to the NACA 63212, Quabeck 2.0/10 R/C sailplane HQ 2010, and GOE 117 airfoils. The resulting inverse design results are shown in Figure 11. Although 29 POD modes are used for the NACA 63212 in Figure 11(a), there is still a small region on the upper surface near the leading edge which cannot be resolved accurately. The situation is worse for the HQ 2010 airfoil. As shown in Figure 11(b), there are some regions on the upper and lower surfaces need to be improved. In Figure 11(c), the design airfoil is still far away from the exact GOE 117 airfoil, indicating that this geometry, which differs considerably from the baseline RAE 2822 airfoil, is not contained in the subspace spanned by the snapshot set considered. From Table 1, the values of the cost J can be seen to be larger than for the Korn airfoil, especially in the case of the HQ 2010 and GOE 117 airfoils. Therefore, a way to improve the design airfoil needs to be developed.

Airfoil	No. modes	J
Korn	1	0.022
Korn	15	0.0047
Korn	29	2.9426e-004
NACA 63212	29	6.2673e-004
HQ 2010	29	0.0061
GOE 117	29	0.0056
NACA 63212 (restart)	43	1.7435e-004
HQ 2010 (restart)	32	2.0622e-004
GOE 117 (restart)	39	6.8127e-004

Table 1 Optimal cost versus number of POD modes for subsonic inverse design cases.

One approach to improve the inverse design results is to increase the richness of the subspace spanned by the POD basis vectors. This can be achieved by including more snapshots in the ensemble. The exact airfoil could be obtained if further snapshots were added to the set; however, this implies some a priori knowledge of the desired result so that appropriate snapshots may be chosen. A better way to improve the design airfoil is proposed in Legresley and Alonso,[2]

where an available design airfoil at some iteration is used as an intermediate baseline, to which some bump functions are added to generate a new set of snapshots. This new snapshot collection is then used to compute a new set of POD modes and thus restart the design procedure. Here, we make use of a similar method for the gappy POD procedure. For the case of the NACA 63212 above, the design airfoil with 29 POD modes is used as an intermediate baseline airfoil, to which 60 bump functions are added to obtain a new collection of 61 snapshots. A similar procedure is used for the intermediate design airfoils shown in Figure 11 for the HQ 2010 and GOE 117 cases, respectively. It can be seen in Figure 12 that the design airfoils now match the exact airfoils very well. In order to obtain a cost on the order 10^{-4}, 43, 32 and 39 POD modes were required for the NACA 63212, HQ 2010, and GOE 117 airfoils, respectively. The costs are shown in Table 1. The results from this restarted gappy POD procedure are much better than those obtained from using the 60-snapshot ensemble above. Moreover, by allowing multiple restarts, this procedure enables the consideration of an inverse design whose geometry differs significantly from that of the baseline airfoil.

Conclusion

The POD basis has been shown to be efficient for capturing relevant flow information for steady transonic aerodynamic applications. By coupling the POD basis with an interpolation method, models are obtained that give accurate flow field predictions. These predictions do not require a projection onto the CFD governing equations, but rather just a collection of flow snapshots that covers the parameter ranges of interest. The interpolation approach is applicable to any problem whose properties of interest are a smooth function of the parameters under consideration. The POD has also been shown to be very effective for reconstructing flow fields from incomplete data sets. While the rate of convergence of the reconstruction depends on the amount of missing data and the structure of the flow field, the method was found to work effectively for all problems considered. Finally, the gappy POD can be used for a simple, yet effective, approach to inverse design of airfoil shapes. By using a systematic restarting procedure, airfoil designs can be effected whose shape is significantly different from those in the original database.

Acknowledgments

This work has been funded by the Singapore-MIT Alliance.

References

[1]Holmes, P., Lumley, J., and Berkooz, G., *Turbulence, Coherent Structures, Dynamical Systems and Symmetry*, Cambridge University Press, Cambridge, UK, 1996.

[2]LeGresley, P. and Alonso, J., "Investigation of Non-Linear Projection for POD Based Reduced Order Models for Aerodynamics," AIAA Paper 2001-0926, presented at 39th Aerospace Sciences Meeting and Exhibit, Reno, NV, 2001.

[3]Sirovich, L. and Kirby, M., "Low-dimensional procedure for the characterization of human faces." Jounal of the Optical Society of America A, 4(3):519-524, 1987.

[4]Fukanaga, K., *Introduction to Statistical Pattern Recognition*, Academic Press, New York, 1972.

[5]Sirovich, L., "Turbulence and the Dynamics of Coherent Structures. Part 1 : Coherent Structures," *Quarterly of Applied Mathematics*, Vol. 45, No. 3, October 1987, pp. 561–571.

[6]Dowell, E., Hall, K., Thomas, J., Florea, R., Epureanu, B., and Heeg, J., "Reduced Order Models in Unsteady Aerodynamics," AIAA Paper 99-1261, 1999.

[7]Hall, K. C., Thomas, J. P., and Dowell, E. H., "Reduced-Order Modeling of Unsteady Small-Disturbance Flows Using a Frequency-Domain Proper Orthogonal Decomposition Technique," AIAA Paper 99-0655, 1999.

[8]Romanowski, M., "Reduced Order Unsteady Aerodynamic and Aeroelastic Models using Karhunen-Loéve Eigenmodes," AIAA Paper 96-194, 1996.

[9]Beran, P. and Silva, W., "Reduced-Order Modeling: New Approaches for Computational Physics," AIAA Paper 2001-0853, 2001.

[10]B. I. Epureanu, Dowell, E. H. and Hall, K., ""A Parametric Analysis of Reduced Order Models of Potential Flows in Turbomachinery Using Proper Orthogonal Decomposition," 2001-GT-0434, Proceedings of ASME TURBO EXPO 2001, New Orleans, Louisiana, June 2001.

[11]Ly, H. V. and Tran, H. T., "Modeling and Control of Physical Processes using Proper Orthorgonal Decomposition," Journal of Mathematical and Computer Modeling, 1999.

[12]Everson, R. and Sirovich, L., "The Karhunen-Loeve Procedure for Gappy Data," J.Opt.Soc.Am., 12: 1657-1664, 1995.

[13]Jameson, A., Schmidt, W., and Turkel, E., "Numerical Solutions of the Euler Equations by Finite Volume Methods Using Runge-Kutta Time-Stepping Schemes," AIAA Paper 81-1259 14th Fluid and Plasma Dynamics Conference, Palo Alto, California, 1981.

[14]Hicks, R. and Henne, P., "Wing Design by Numerical Optimization." Journal of Aircraft, 15:407-412, 1978.

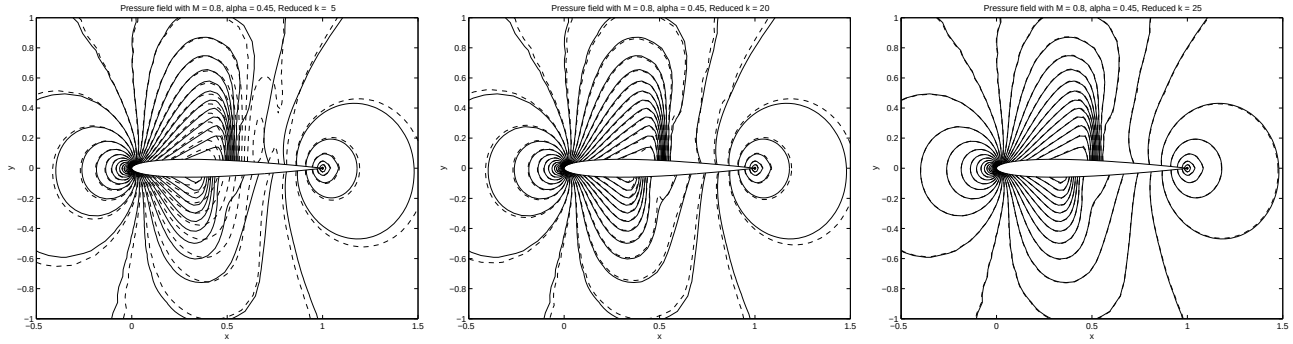

a) **b)** **c)**

Fig. 1 Comparison of predicted pressure contours (dash) and CFD pressure contours (solid) for a Mach number of 0.8 and angle of attack of 0.45°; (a) five POD eigenfunctions, (b) twenty POD eigenfunctions, (c) 25 POD eigenfunctions.

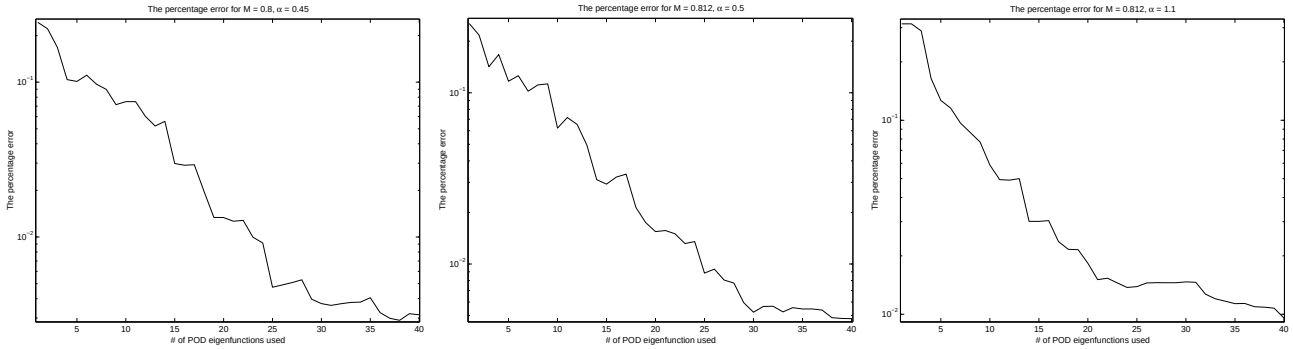

a) **b)** **c)**

Fig. 2 Variation of percentage error versus the number of POD eigenfunctions in log scale; (a) M = 0.8 and $AOA = 0.45^{\circ}$, (b) M = 0.812 and $AOA = 0.5^{\circ}$, (c) M = 0.812 and $AOA = 1.1^{\circ}$.

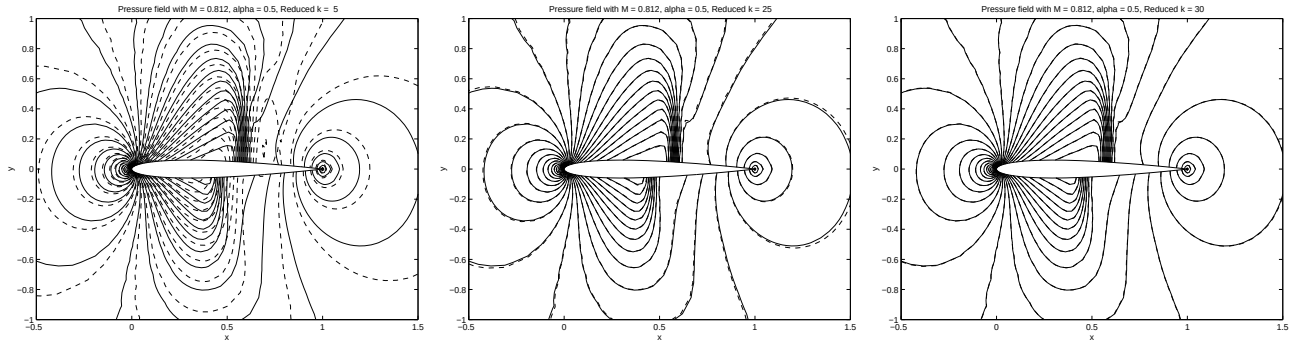

a) **b)** **c)**

Fig. 3 Comparison of predicted pressure contours (dash) and CFD pressure contours (solid) for a Mach number of 0.812 and angle of attack of 0.5°; (a) five POD eigenfunctions, (b) 25 POD eigenfunctions, (c) thirty POD eigenfunctions.

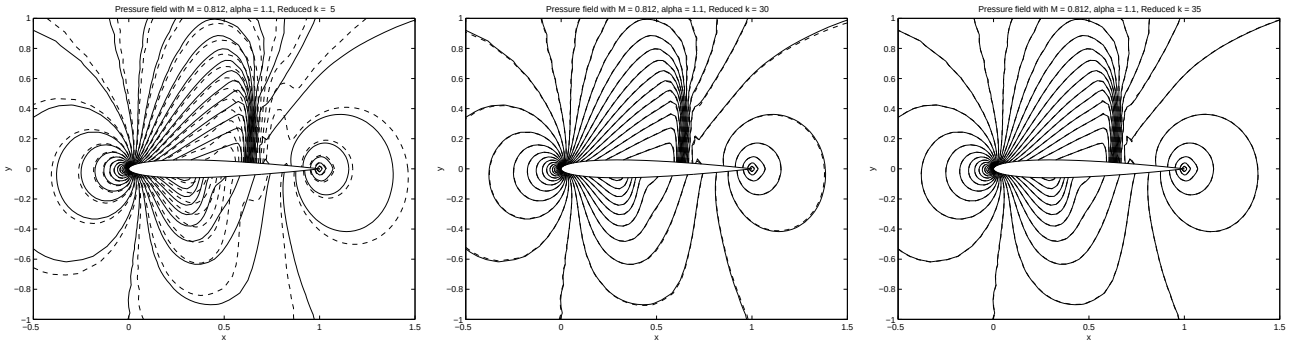

a) **b)** **c)**

Fig. 4 Comparison of predicted pressure contours (dash) and CFD pressure contours (solid) for a Mach number of 0.812 and angle of attack of 1.1°; (a) five POD eigenfunctions, (b) thirty POD eigenfunctions, (c) 35 POD eigenfunctions.

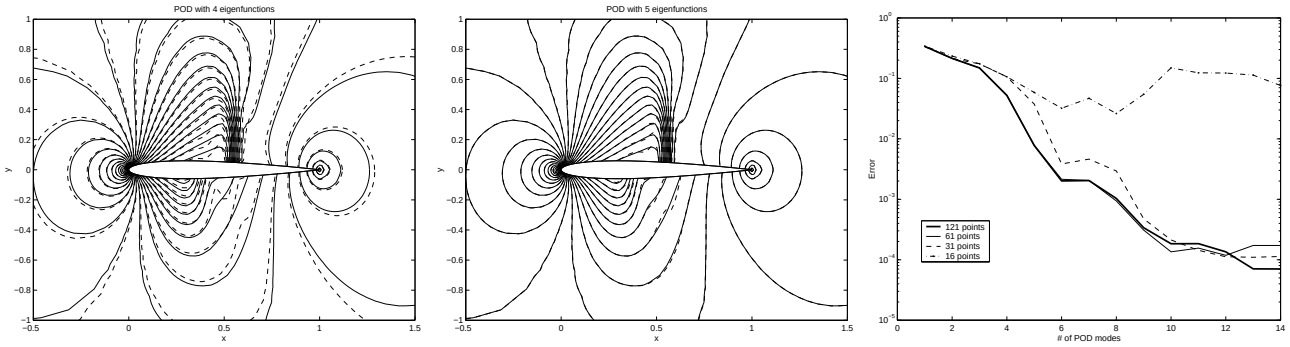

a) **b)** **c)**

Fig. 5 Reconstruction of the pressure field from airfoil surface pressure distribution (dash) compared with the original CFD contours (solid); (a) Reconstruction with four POD eigenfunctions; (b) reconstruction with five POD eigenfunctions; (c) the 2-norm of the pressure reconstruction error versus the number of POD modes with 16, 31, 61 and 121 equally spaced surface pressure measurements.

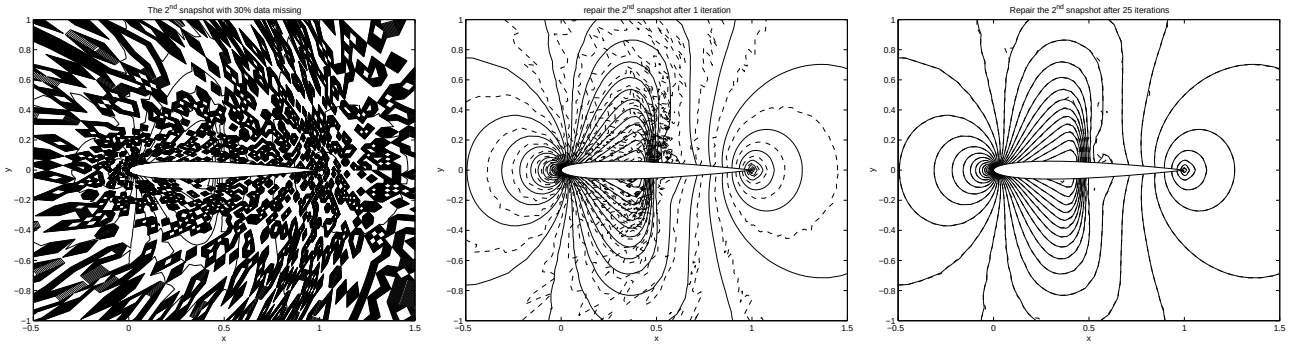

a) **b)** **c)**

Fig. 6 Reconstruction of the second snapshot (dash), compared with the original contours (solid); (a) The second snapshot with 30% data missing, (b) Reconstruction after one iteration, (c) Reconstruction after 25 iterations.

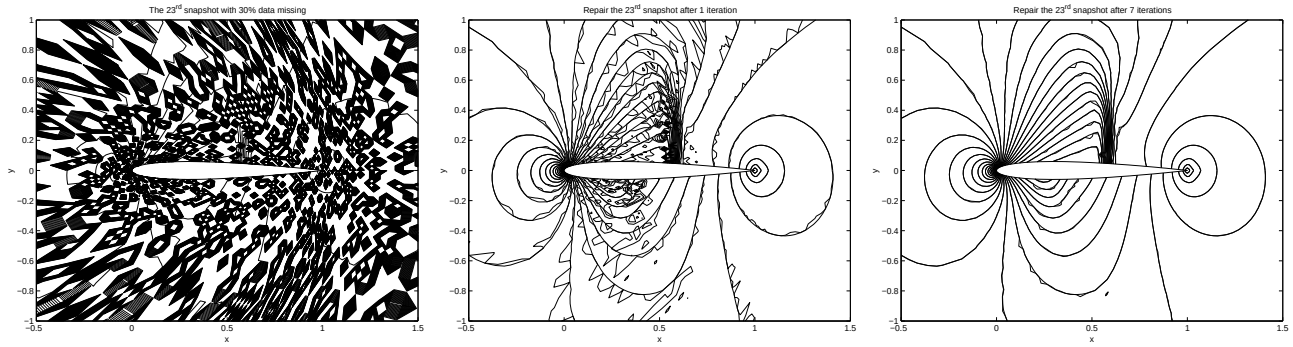

a) **b)** **c)**

Fig. 7 Reconstruction of the 23^{rd} snapshot (dash), compared with the original contours (solid); (a) The 23^{rd} snapshot with 30% data missing, (b) Reconstruction after one iteration, (c) Reconstruction after seven iterations

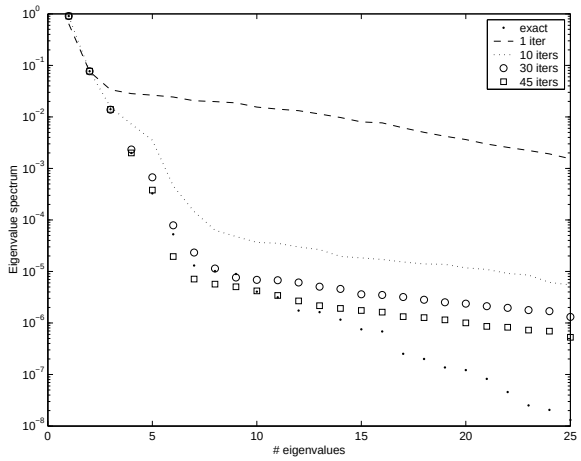

Fig. 8 The eigenvalue spectrum for construction of the POD basis from an incomplete snapshot set. Shown are the POD eigenvalues at various stages in the iterative process.

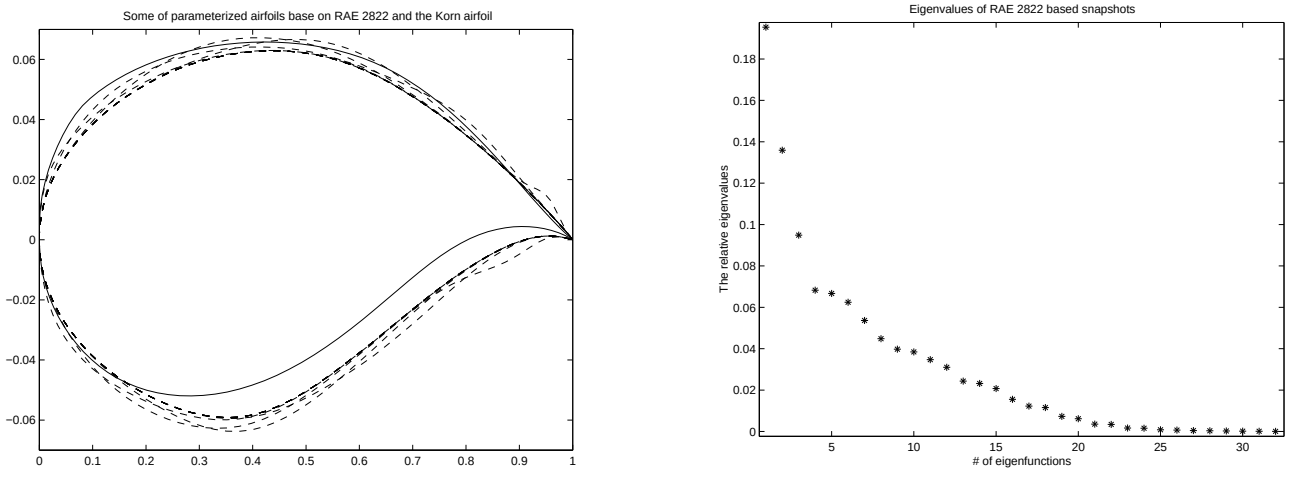

a) **b)**

Fig. 9 The airfoil snapshots and corresponding POD eigenvalues; (a) Parameterized airfoils based on RAE 2822 (dash) and the Korn airfoil (solid), (b) The relative eigenvalues from RAE 2822 based snapshots

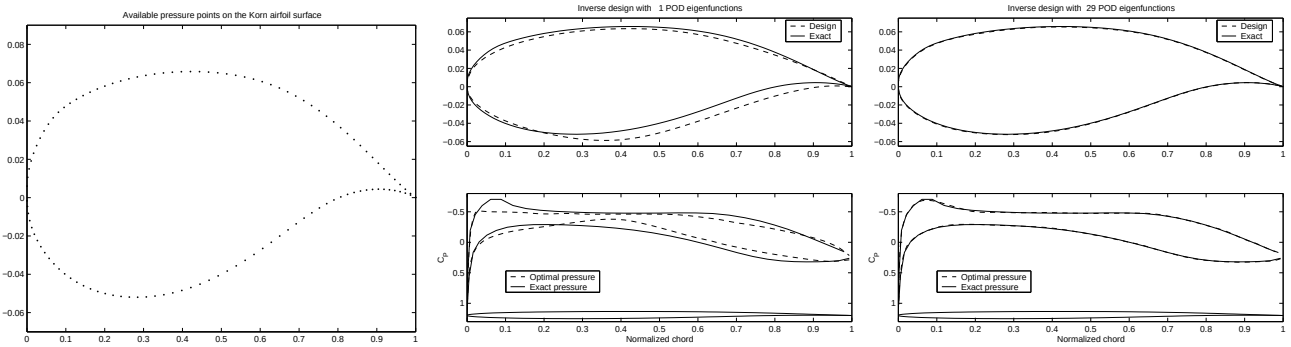

a) **b)** **c)**

Fig. 10 Inverse design of the Korn airfoil using gappy POD. $M = 0.5$, snapshots based on RAE 2822; (a) The available pressure points on the surface of the Korn airfoil, (b) The exact Korn airfoil (solid) and the design airfoil (dash) with one mode, (c) The exact Korn airfoil (solid) and the design airfoil (dash) with 29 modes.

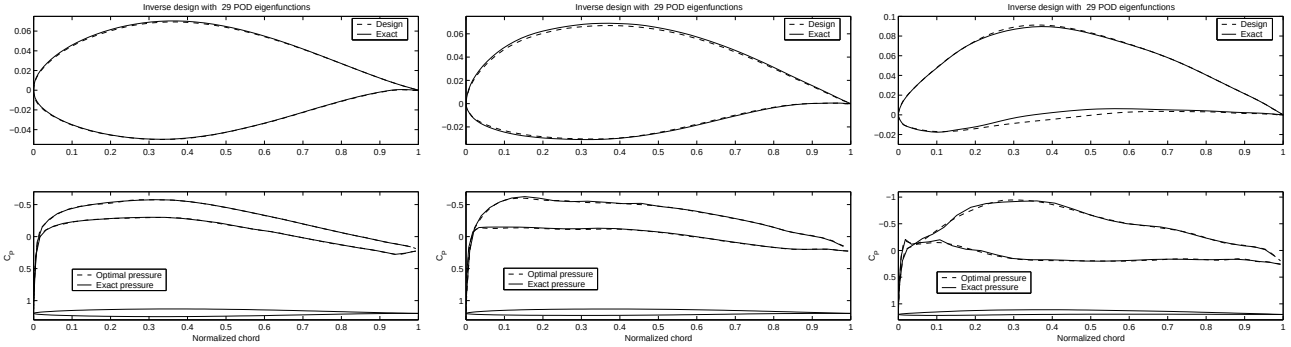

a) **b)** **c)**

Fig. 11 Inverse design of the NACA 63212, HQ 2010 and GOE 117 airfoils using gappy POD. $M = 0.5$, snapshots based on RAE 2822; (a) The exact NACA 63212 airfoil (solid) and the design airfoil (dash) with 29 modes, (b) The exact HQ 2010 airfoil (solid) and the design airfoil (dash) with 29 modes, (c) The exact GOE 117 airfoil (solid) and the design airfoil (dash) with 29 modes.

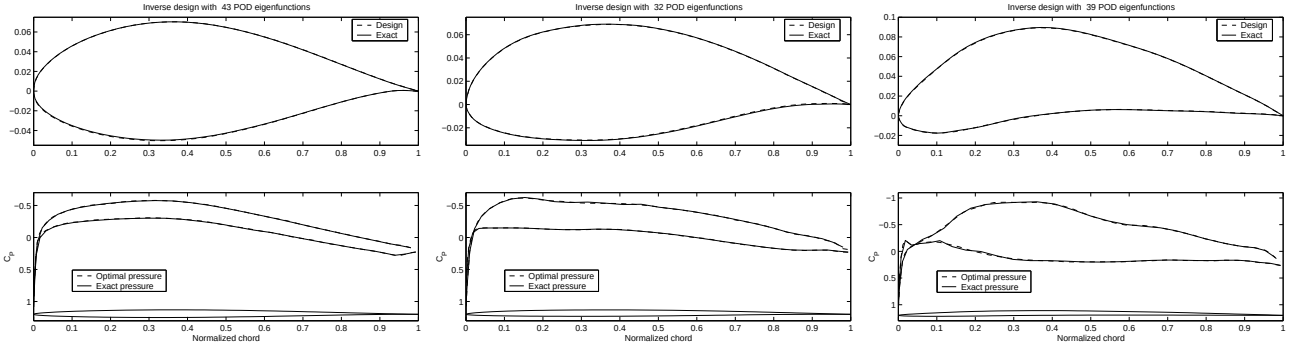

a) **b)** **c)**

Fig. 12 Inverse design of the NACA 63212, HQ 2010 and GOE 117 airfoils using restarted gappy POD. $M = 0.5$, original snapshots based on RAE 2822, restarted snapshots based on intermediate airfoils shown in Figure 11; (a) The exact NACA 63212 airfoil (solid) and the design airfoil (dash) with 43 modes, (b) The exact HQ 2010 airfoil (solid) and the design airfoil (dash) with 29 modes, (c) The exact GOE 117 airfoil (solid) and the design airfoil (dash) with 34 modes.